A Global Traveling Wave on Venus

Michael D. Smith, Peter J. Gierasch, Paul J. Schinder

The dominant large-scale pattern in the clouds of Venus has been described as a "Y" or "Ψ" and tentatively identified by earlier workers as a Kelvin wave. A detailed calculation of linear wave modes in the Venus atmosphere verifies this identification. Cloud feedback by infrared heating fluctuations is a plausible excitation mechanism. Modulation of the large-scale pattern by the wave is a possible explanation for the Y. Momentum transfer by the wave could contribute to sustaining the general circulation.

The general circulation on Venus is dominated by spin of the atmosphere. The direction of the spin is the same as that of the planet but about 50 times faster at cloud-top level, approximately 70 km above the surface. The atmosphere is composed primarily of CO_2, and the pressures at the surface and at the cloud tops are ~90 bars and 50 mbar, respectively (*1*). The planet rotates with a period of 243 days, and the cloud tops with a period of 4 or 5 days. The detailed rotational structure shows jets at mid-latitudes (*2*) and vertical shear (*3*) that correlates with the vertical temperature gradient, but to a first approximation the rotation increases linearly with height and each shell of atmosphere is in rigid body rotation. This puzzling configuration is not understood, because countergradient momentum fluxes (Reynold's stresses) within the fluid are required to maintain the flow against dissipative processes.

The Venus clouds are featureless in visible light but show contrast in the ultraviolet (Fig. 1). The large-scale pattern has been described as a traveling Ψ or Y (turned sideways). It rotates with a period of 4 or 5 days and is global in scale (*4*), with a strong component at a zonal wave number of unity. The wave sometimes moves more rapidly than the equatorial wind speed and sometimes more slowly, but the speed difference is less than 20%. The true wind speed is indicated by the motion of small-scale blotches and wisps in the clouds (*5*). The visibility of the Y varies, and sometimes, although rarely, it is not apparent at all. Exhaustive analysis of Pioneer Venus orbiter images has revealed that the wave also manifests itself in perturbations of the zonal wind speed, with an amplitude of several meters per second and with a particular phasing relative to the albedo pattern (*6*).

Time-lapse images from the Galileo spacecraft (*7*) reveal that the wind oscillation was particularly strong at the time of the flyby (February 1990), with an amplitude of about 10 m s^{-1} (*8*). Figure 1 displays additional zonal (west-east) velocities that we have measured in order to examine the dependence of the amplitude on latitude. We have found that meridional (south-north) wave velocities are too small (less than 3 m s^{-1}) to extract from the data with present techniques.

Infrared monitoring from Earth at the flyby time revealed that the deep cloud varied spatially in optical thickness by as much as 25%, and that the variation contains a strong component with wave number equal to one (*9*). The velocity of the large-scale cloud disturbance is greater than that of small-opacity patches in the deep cloud, and we suggest that the high velocity is associated with the same global wave that is apparent in the cloud-top ultraviolet markings.

Belton *et al.* (*5*) speculated that the large-scale wave on Venus is analogous to a Kelvin mode, which is an internal gravity wave modified by Coriolis effects. This mode is confined to low latitudes and has zonal velocity perturbations but no meridional velocities. DelGenio and Rossow (*6*) confirmed a velocity field consistent with Kelvin waves in an extensive study of Pioneer Venus images. Covey and Schubert (*10*) calculated the structure of global-scale Kelvin waves on Venus but did not account for the excitation of the wave or the coherence of the Y with time. We report here calculations of the detailed structure of planetary waves on Venus. We find that there is a Kelvin-like mode, although global in scale, whose propagation speed agrees with the observations. Moreover, we find that radiative heating variations, caused by the influence of the wave on the cloud deck, can lead to a feedback that amplifies the wave and that a modulation of the large-scale cloud pattern by the wave can account for the Y feature.

Our mathematical model is similar to that used by Covey and Schubert (*10*). The equations of motion are linearized about a basic state in which the zonal velocity is proportional to the cosine of the latitude at each height; that is, each atmospheric shell

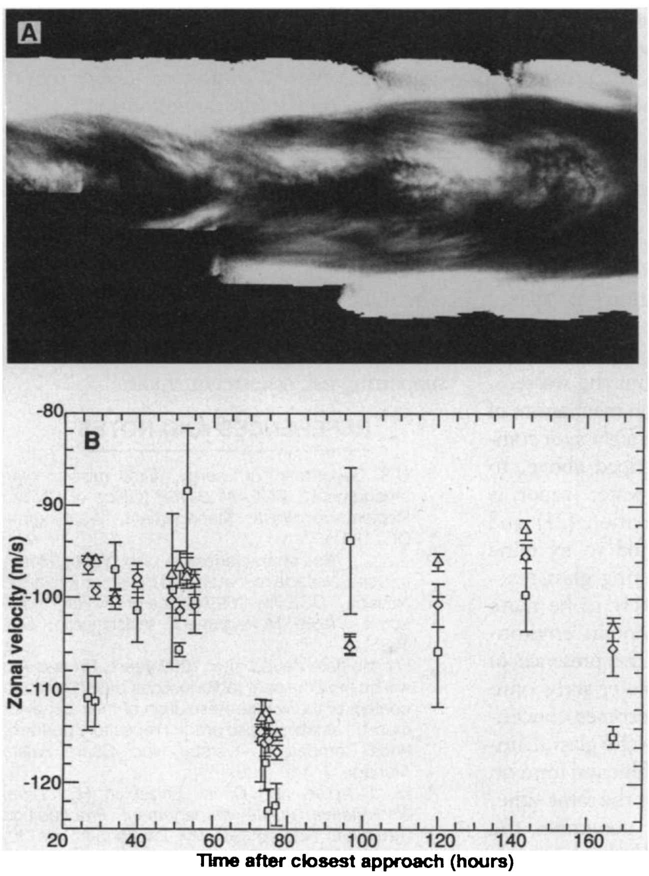

Fig. 1. (**A**) Rectangular projection of a set of Galileo images taken as the cloud system rotated under the spacecraft. (**B**) Wind measurements from the Galileo data (*8*). The data are shown as a time series for three different latitude bins: The triangles include measurements taken between 0° and 15° north, the diamonds between 15° and 30° north, and the squares between 30° and 45° north. A cyclical variation with an amplitude of ~10 m s^{-1} and a period of ~4 days is observed in all bins.

M. D. Smith and P. J. Gierasch, Astronomy Department, Space Sciences Building, Cornell University, Ithaca, NY 14853.
P. J. Schinder, Laboratory for Extraterrestrial Physics, National Aeronautics and Space Administration (NASA) Goddard Space Flight Center, Code 693, Greenbelt, MD 20771.

rotates as a rigid body. The velocity profile in height, and the temperature and stability profiles, are accurate reproductions of actual measurements (*11*). The vertical force balance is assumed to be hydrostatic, because large-scale waves are being examined. Radiative damping varies with height in a realistic way (*12*). Vertical diffusion of both heat and momentum are included. The diffusion coefficients are small except near the top of the model atmosphere, at 25 pressure scale heights, or at an altitude of ~145 km, where they are artificially made large to absorb upward energy propagation. This is done to simulate dissipative processes that are known to act in the upper atmosphere. The bottom boundary condition is a rigid surface. A broad, smooth external thermal forcing over the altitude range 20 km < z < 50 km is used. Solutions are harmonic in time and are represented spatially as a series of spherical harmonics whose coefficients vary in height. These are evaluated at grid points. Because of the vertical wind shear in the basic state, the variables do not separate in their latitude and height dependence. Typically, 500 grid points used in the vertical and spherical harmonics up to $Y_{m,11}$ are retained.

Free modes of the system would be characterized by three numbers: (i) the longitudinal wave number m, (ii) a latitudinal count of nodes n, and (iii) a vertical index that measures the complexity of the mode in the radial direction. Each of these modes would have a characteristic frequency. Because the system always contains a certain amount of dissipation, our mathematical model does not have "free" modes. However, if we impose a forcing over a range of frequencies and examine the response of the system, we find maxima at a certain set of frequencies, analogous to those of the free modes that an idealized closed system would exhibit. The complete family of modes shows horizontally propagating acoustic modes at high frequencies and gravity waves at low frequencies. Of particular interest are those modes that have longitudinal velocities close to that of the mean wind at cloud-top level because these are candidates for explaining the observed traveling mode. These turn out to be the lowest gravity modes, those with a small number of nodes in the vertical and in the horizontal.

Primarily because of the dissipation at the top of the system, none of these modes is highly tuned. The wave energy divided by the energy loss per period, or Q, is relatively small, on the order of five. Because the period is about 4 days, these modes will decay with a characteristic time of about 20 days. Thus, a process of excitation must be identified. Cloud feedback is a possibility. Measurements by Pioneer Venus probes show that the densest part of the Venus clouds is at an altitude of ~50 km, near their base (*13*). We hypothesize that vertical motions associated with the large-scale wave lead to evaporation (for downward motion, which produces compressional heating) or condensation (upward). In the optically thick regime (*14*), the infrared heat flux is inversely proportional to the cloud number density. Thus evaporation of particles will increase the upward radiative flux at the cloud base, leading to an increased heating just above the cloud base and to cooling just below it. Solar heating is of secondary importance at these depths, because the solar flux is attenuated by a factor of about 5 from its cloud-top value (*15*).

The cloud feedback can be parameterized if we add to the mathematical model a heating of the form (*16*)

$$Q' = \beta f(z) \frac{T}{t_R} \frac{\delta z}{H} \quad (1)$$

where $f(z)$ is a profile function whose maximum is unity and whose shape and width are chosen to simulate the cloud effect, T is the temperature, t_R is the radiative time constant for temperature perturbations with a length scale of a scale height (*12*), δz is the vertical displacement associated with the wave, and H is the scale height of the atmosphere at cloud level; β sets the amplitude of the effect and is a parameter to be varied. This formulation is used to study cloud feedback heating caused by vertical motions. Other possibilities, such as cloud feedback heating caused by temperature perturbations, are not considered here. We have experimented with a detailed radiative transfer model to determine the effect of removing the bottom 2 km of the cloud deck. Guided by these results, we have chosen a smooth $f(z)$ with maximum modulus equal to unity, $f(z) > 0$ for 45 km < z < 49 km, $f(z) < 0$ for 49 km < z < 53 km, and $f(z) = 0$ elsewhere. For $\beta = 1$, a vertical displacement of one scale height produces a heating rate equal to the local temperature divided by the local radiative time constant. This means that a displacement of one scale height changes the radi-

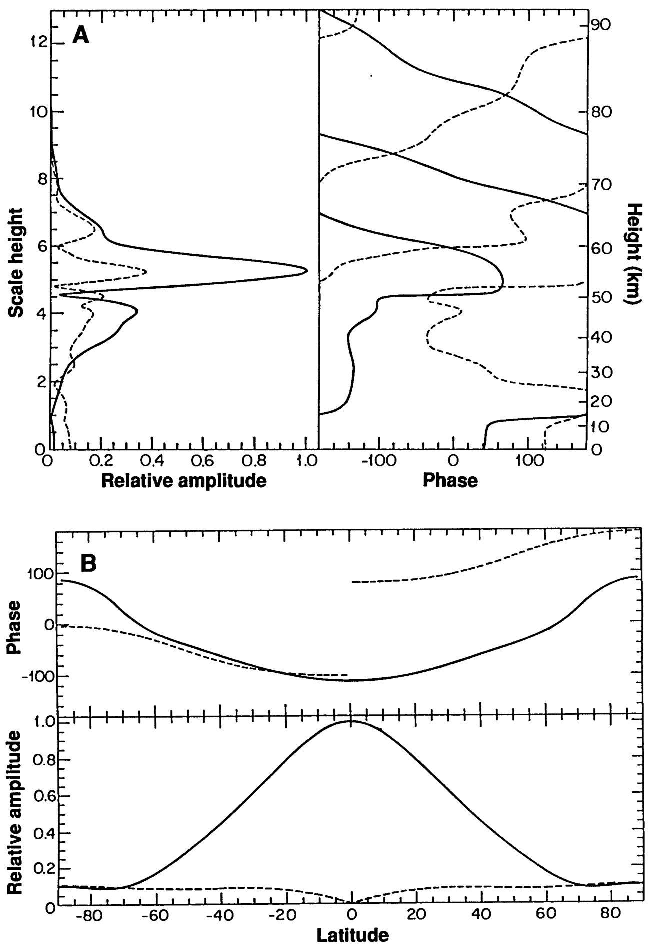

Fig. 2. Structure of the most unstable wave mode, with β adjusted to give zero growth rate. This structure is independent of the artificial external thermal forcing used to excite the system and is very nearly independent of β. For the neutral mode there is a resonance, and the free response has been isolated by subtracting two forced solutions in the immediate neighborhood of the resonance frequency. This has the effect of retaining only that part of the solution whose amplitude peaks near the resonance. This free response is then independent of the form of the external thermal forcing used, but the scaling is arbitrary. The solid line shows zonal velocities and the dashed line shows meridional velocities. In (**A**) the zonal velocity is taken at the equator, and the meridional velocity is taken at 30° north. The amplitude of the meridional velocity component has been multiplied by ten. The phases are shown relative to the longitude at which the zonal or meridional oscillation is completely real and positive (eastward or southward, respectively). In (**B**) both profiles are taken at a pressure scale height of 6.5 (63 km). Above ~55 km, the zonal velocity profile shows propagation upward; below 55 km, the wave is standing. The 180° changes in phase near 15 and 50 km are nodes.

ative flux by its own order of magnitude. If the cloud feedback effect occurs in a layer of thickness less than a scale height, as indicated by our $f(z)$, then values of β greater than unity are physically possible.

For $m = 1$ and $\beta = 1.217$, a moderately large but still physically reasonable value for the instability parameter, there is a neutrally stable mode whose phase speed is -102 m s^{-1}. The effect of β on the growth rate of the wave is roughly linear. Values of β larger than 1.217 will produce instability.

The most unstable mode has two nodes in the vertical and no nodes in the horizontal (see Fig. 2). The phase speed of -102 m s^{-1} is consistent with the wave observed in the Galileo images, although there is probably about a 20% uncertainty in the Galileo wave estimate because an observation period of only 7 days was used. The wave amplitude in zonal velocity is about five times the wave amplitude in meridional velocity at the cloud-top level, consistent with the Galileo wind measurements. The calculated zonal velocity amplitude is largest at the equator and has a full width at half maximum of about 70° (35°S to 35°N). Dynamically this wave is in the Kelvin class (*17*), as anticipated by DelGenio and Rossow (6), but global in scale. It propagates in the direction of the atmospheric rotation, the restoring force is gravity, and rotation acts to confine the amplitude in latitude.

The vertical structure of the wave shows strong attenuation above an altitude of ~60 km, suggesting that the visibility of the wave may depend on exactly where the cloud tops are located at a particular instant. There is evidence that the location of the Venus cloud tops is variable (*18*). The maximum amplitude of the zonal velocity fluctuation associated with the wave is near 55 km. We would anticipate that wind variations should be detectable in ground-based near-infrared images of Venus. A typical zonal velocity fluctuation observed at cloud top in the violet is 5 m s^{-1} (6), and the fluctuation at cloud base should be several times larger. Current near-infrared measurements (9) show large scatter in zonal velocity and can neither confirm nor rule out the presence of a wave with an amplitude of 25 m s^{-1}.

A spectrum showing the rates of energy inputs and outputs for the case with $\beta = 1.217$ (neutral stability) is shown in Fig. 3. For the most unstable mode (-102 m s^{-1}) the heating caused by cloud feedback is the largest source of energy input, while thermal diffusion and radiative damping act as energy sinks. Other sinks of energy, including friction and momentum coupling to the mean flow, are smaller.

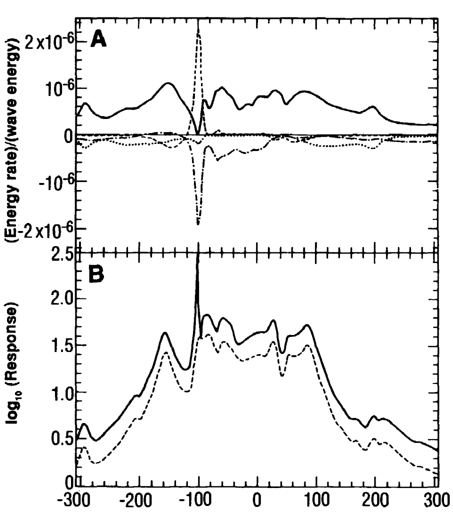

Fig. 3. (**A**) Spectrum of $m = 1$ wave energetics. The solid line shows the external thermal heating rate, the dashed line the cloud heating rate, the dash-dot line the rate of thermal diffusion, and the dotted line the rate of cooling by radiation. The cloud heating is only important in the region near the most unstable mode. At that frequency the heating rate from the external source is zero, indicating a neutral mode, and cloud heating is balanced primarily by thermal diffusion. For this value of β, all other wave modes show decay in time. (**B**) The response of the system as a function of frequency. The solid line shows the response with β set to give zero growth rate to the mode at -102 m s^{-1}. The dashed line shows the response when $\beta = 0$. The $\beta = 0$ spectrum has been offset downward by 0.25 unit. Shown without the offset, the two curves would be indistinguishable except near the frequency of the neutrally stable mode.

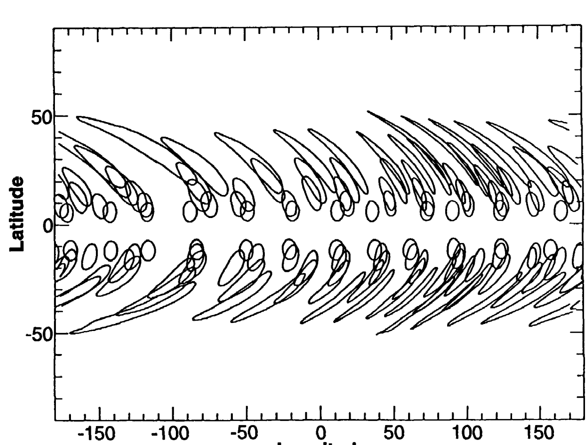

Fig. 4. Simulated cloud pattern. Circular bubbles are released at random longitudes near the equator and are then advected under the influence of the mean flow with an added wave. The mean flow is as measured from Galileo images (*8*) and includes poleward drift and mid-latitude jets.

For higher values of m, instabilities also exist. The critical value of β for the onset of instability is nearly independent of m for $m < 10$ and becomes large for $m > 10$. Thus we expect smaller scale modes to exist in addition to the $m = 1$ mode. The vertical structure of modes for $m > 1$ is confined to deeper levels and is probably not visible at 70 km where the violet features are formed. At cloud base the higher modes may have significant amplitude, and indeed small-scale structure is observed in the near-infrared (9).

An important property of a wave is the degree and sense of correlation between zonal, meridional, and vertical motions. We calculated the correlations and associated momentum fluxes of zonal angular momentum through surfaces of constant latitude and height for the most unstable mode. The lower atmosphere and cloud-top levels are accelerated at the expense of the forcing level, and the equator is accelerated at the expense of mid-latitudes. This is the correct sense of angular momentum transport needed to contribute to the maintenance of the cloud-top superrotation. The absolute correlation of the wave velocities is large, indicating that the direction of momentum transport is not sensitive to details in the vertical and horizontal structure of the wave.

In an earlier paper we postulated that the mid-latitude streaky pattern of clouds seen on Venus is attributable to the formation of clouds near the equator and the subsequent poleward advection and shearing of the clouds by the winds (*19*). Expanding on that idea, we performed a numerical experiment in which we released clouds at random locations near the equator and let the measured Galileo Venus mean wind (8) and a superimposed wave advect them forward. Figure 4 shows the results of this experiment based on the most unstable mode found above and typical values for the zonal and meridional wave amplitudes and phasing (*20*). We see a modulation of the cloud shapes and orientations of the cloud streaks at mid-latitudes caused by the wave, which are similar to those seen in the observations (Fig. 1). This suggests that the Ψ or Y feature is caused by the wave modulating the advective patterns of the clouds.

The oscillation of wind velocities seems to be sporadic in nature. In the Galileo data set the wave was very pronounced (8), but at times during the Pioneer Venus mission no wave was detected (6). Our calculation shows that the wave amplitude of the most unstable mode varies strongly with height. It is possible that variation in the level of the observed cloud top contributes to the irregularity of the observed wind oscillations. A variation in the zonal wind profile or in the trapping properties of the atmosphere could also cause the wave to appear sometimes but not at other times. Our analysis of Pioneer Venus observations shows that velocity oscillations may appear for a few days, disappear, and then reappear with a phasing unrelated to the previously observed oscillation. This sort of behavior is consistent with the low Q associated with the waves in our computation.

Energy sources other than cloud feedback are possible. Instability of horizontal shear is an obvious candidate excluded by assumption from the modeling reported here. The key point is that a low-order global wave mode that appears to have the correct kinematic properties has been identified. In the absence of a forcing mechanism, it is estimated to decay with about a 20-day time scale. Cloud feedback seems to have the right magnitude to provide the forcing and also seems to pick out the correct phase velocity for the most unstable mode, but we have not excluded other possibilities for excitation.

REFERENCES AND NOTES

1. A. Seiff *et al.* [*J. Geophys. Res.* **85**, 7903 (1980)] reported the thermodynamic structure of the Venus atmosphere as measured by the NASA Pioneer Venus probes in 1979. Optical properties of the cloud tops were discussed by K. Kawabata *et al.* (*ibid.*, p. 8129).
2. The latitudinal profile of cloud-top winds varies over time, and the mid-latitude jets are sometimes almost absent. The 1974 profile was measured by S. S. Limaye and V. E. Suomi [*J. Atmos. Sci.* **38**, 1220 (1981)]; the 1979 profile by W. B. Rossow, A. D. DelGenio, S. S. Limaye, and L. D. Travis [*J. Geophys. Res.* **85**, 8107 (1980)]; and the 1982 profile by S. S. Limaye, C. Grassotti, and M. J. Kuetemeyer [*Icarus* **73**, 193 (1988)]. Profiles for 1980 and 1983 were measured by us and are presented in (*19*).
3. The vertical wind profile, based on tracking Pioneer Venus probe drifts, was found to be similar at four widely separated locations [C. C. Councelman III, S. A. Gourevitch, R. W. King, G. B. Loriot, *J. Geophys. Res.* **85**, 8026 (1980)].
4. M. J. S. Belton, G. R. Smith, D. A. Elliott, K. Klaasen, G. E. Danielson, *J. Atmos. Sci.* **33**, 1383 (1976); W. B. Rossow, A. D. DelGenio, S. S. Limaye, L. D. Travis, *J. Geophys. Res.* **85**, 8107 (1980).
5. M. J. S. Belton, G. R. Smith, G. Schubert, A. D. DelGenio, *J. Atmos. Sci.* **33**, 1394 (1976).
6. A. D. DelGenio and W. B. Rossow, *ibid.* **47**, 293 (1990).
7. A collection of articles on the Galileo flyby and the associated ground-based campaign was published in *Science* [**253**, 1516–1550 (1991)].
8. M. J. S. Belton *et al.*, *ibid.*, p. 1531.
9. See D. Crisp *et al.*, *ibid.*, p. 1538, and references therein.
10. C. Covey and G. Schubert, *J. Atmos. Sci.* **39**, 2397 (1982).
11. A convenient parameterization of the basic state wind and temperature profiles in the Venus atmosphere was introduced by R. E. Young *et al.*, *ibid.* **44**, 2628 (1987). We experimented with the sensitivity of wave modes to alterations in the basic state. The lowest modes, which turn out to be the ones of principal interest, are not highly sensitive to variations of the basic state that are consistent with observational variability or uncertainty.
12. We fitted a smooth function to the radiative time constant estimates by D. Crisp [*Icarus* **77**, 391 (1989)] for altitudes above ~60 km, and for a disturbance with vertical wavelength of ~20 km, roughly consistent with our calculated results. At altitudes less than 60 km, we followed the estimates by J. B. Pechmann and A. P. Ingersoll [*J. Atmos. Sci.* **41**, 3290 (1984)].
13. R. G. Knollenberg and D. M. Hunten [*J. Geophys. Res.* **85**, 8039 (1980)] presented data from the Pioneer Venus particle size spectrometer experiment.
14. R. G. Knollenberg *et al.* (*ibid.*, p. 8059) calculated optical depths from the data presented in (*13*). There are about 20 optical depths at visible wavelengths within a layer that is 7 km thick (this is approximately a pressure scale height). M. G. Tomasko *et al.* (*ibid.*, p. 8187) estimated cross sections in the thermal infrared to be about half of those in the visible, which places the cloud in the optically thick regime.
15. M. G. Tomasko, L. R. Doose, P. H. Smith, A. P. Odell, *ibid.*, p. 8167.
16. Cloud instabilities of this type have been studied by P. J. Gierasch, A. P. Ingersoll, and R. T. Williams [*Icarus* **19**, 473 (1973)] and by S. J. Ghan [*J. Atmos. Sci.* **46**, 2529 (1989)].
17. M. S. Longuet-Higgins [*Proc. R. Soc. London Ser. A* **262**, 511 (1968)] discussed the horizontal structure of waves on a rotating planet. We used his calculations to check our numerical procedure.
18. L. W. Esposito, *Science* **223**, 1072 (1984).
19. P. J. Schinder, P. J. Gierasch, S. S. Leroy, M. D. Smith, *J. Atmos. Sci.* **47**, 2037 (1990).
20. The phasing is chosen so that the maximum eastward perturbation in zonal velocities is in phase with the maximum northward perturbation in meridional velocities. The zonal wave amplitude is 10 m s^{-1}, and the meridional wave amplitude is 2 m s^{-1}. This phasing and amplitude are consistent with the results of our computation and with observations.

21. This work was supported by the NASA Galileo Project, the NASA Pioneer Venus Project, and the NASA Planetary Atmospheres Program. The computations were performed at the Cornell National Supercomputer Facility, which is supported by Cornell University, IBM, and the National Science Foundation. We thank M. J. S. Belton, C. Leovy, and two anonymous referees for helpful criticism.

24 December 1991; accepted 9 March 1992

Protein Solvation in Allosteric Regulation: A Water Effect on Hemoglobin

Marcio F. Colombo,* Donald C. Rau, V. Adrian Parsegian

The oxygen affinity of hemoglobin varies linearly with the chemical potential of water in the bathing medium, as seen from the osmotic effect of several neutral solutes, namely sucrose, stachyose, and two polyethyleneglycols (molecular weights of 150 and 400). The data, analyzed either by Wyman linkage equations or by Gibbs-Duhem relations, show that ~60 extra water molecules bind to hemoglobin during the transition from the fully deoxygenated tense (T) state to the fully oxygenated relaxed (R) state. This number, independent of the nature of the solute, agrees with the difference in water-accessible surface areas previously computed for the two conformations. The work of solvation in allosteric regulation can no longer go unrecognized.

The regulation of protein or enzymatic activity is often accomplished through the control of equilibrium among allosteric conformations. Differences in binding affinities of small effector molecules to specific regulatory sites among these conformations modulate this equilibrium. For hemoglobin (Hb), the prototypic allosteric protein, equilibrium between R and T conformations, and consequently its oxygen (O_2) affinity, is modulated by the binding of several small molecules and ions, such as H^+, CO_2, phosphates, and Cl^-. The structures of the two limiting conformations show that several direct contacts between subunits are broken and exposed to solvent during the transition from deoxy T state to the fully oxygenated R state (*1*). This change in structure implies a difference in hydration or water binding between the two conformations. However, the energetic consequences of solvation regulating protein activity are usually neglected.

Such water sensitivity can, in fact, be probed through the dependence of O_2 affinity on water activity or, equivalently, osmotic pressure. This "osmotic stress" method (*2*) has been used to measure intermolecular forces (*3*), to map the thermodynamics of Hb S assembly (*4*), to measure the change in aqueous volume of a large, voltage-gated ionic channel (*5*), and to modify the electron transfer reaction in cytochrome C oxidase (*6*).

The linkage between O_2 uptake and ligand concentration is most often analyzed by relations developed by Wyman (*7*). The

M. F. Colombo and D. C. Rau, Laboratory of Biochemistry and Metabolism, National Institute of Diabetes and Digestive and Kidney Diseases, National Institutes of Health, Bethesda, MD 20892.
V. A. Parsegian, Physical Sciences Laboratory, Division of Computer Research and Technology and Laboratory of Biochemistry and Metabolism, National Institute of Diabetes and Digestive and Kidney Diseases, National Institutes of Health, Bethesda, MD 20892.

*On leave from Departamento de Física, IBILCE-UNESP, São José do Rio Prêto, São Paulo, Brazil.